



Improved sensitivity of lateral flow assay using paper-based sample concentration technique



Ruihua Tang^{a,b,c,d}, Hui Yang^{a,b,*}, Jane Ru Choi^{c,d,e}, Yan Gong^{c,d}, Jie Hu^{c,d}, Shangsheng Feng^{c,d}, Belinda Pingguan-Murphy^e, Qibing Mei^{a,b}, Feng Xu^{c,d,**}

^a School of Life Sciences, Northwestern Polytechnical University, Xi'an 710072, PR China

^b Key Laboratory for Space Bioscience and Biotechnology, Northwestern Polytechnical University, Xi'an 710072, PR China

^c The Key Laboratory of Biomedical Information Engineering of Ministry of Education, School of Life Science and Technology, Xi'an Jiaotong University, Xi'an 710049, PR China

^d Bioinspired Engineering and Biomechanics Center (BEBC), Xi'an Jiaotong University, Xi'an 710049, PR China

^e Department of Biomedical Engineering, Faculty of Engineering, University of Malaya, Lembah Pantai, 50603 Kuala Lumpur, Malaysia

ARTICLE INFO

Article history:

Received 6 November 2015

Received in revised form

1 February 2016

Accepted 5 February 2016

Available online 6 February 2016

Keywords:

Lateral flow assay

Dialysis-based concentration

Paper-based device

HIV

MYO

ABSTRACT

Lateral flow assays (LFAs) hold great promise for point-of-care testing, especially in resource-poor settings. However, the poor sensitivity of LFAs limits their widespread applications. To address this, we developed a novel device by integrating dialysis-based concentration method into LFAs. The device successfully achieved 10-fold signal enhancement in Human Immunodeficiency Virus (HIV) nucleic acid detection with a detection limit of 0.1 nM and 4-fold signal enhancement in myoglobin (MYO) detection with a detection limit of 1.56 ng/mL in less than 25 min. This simple, low-cost and portable integrated device holds great potential for highly sensitive detection of various target analytes for medical diagnostics, food safety analysis and environmental monitoring.

© 2016 Elsevier B.V. All rights reserved.

1. Introduction

Lateral flow assays (LFAs) have found widespread applications in disease diagnosis [1], food safety analysis [2] and environmental monitoring [3] in resource-poor settings. As compared to standard laboratory technologies such as enzyme-linked immunosorbent assay (ELISA) [4] and polymerase chain reaction (PCR) [5] which are time-consuming, high cost and require skilled workers, LFAs are simple-to-use, rapid, low-cost and portable [6–8]. LFAs have been used for detection of various targets, such as nucleic acids [9], proteins [10], viruses [11], bacterium [12], cells etc. However, the poor sensitivity of LFAs limits their further applications [6].

Various approaches have been developed to improve the assay itself to enhance the LFAs sensitivity, such as enzyme-based signal enhancement techniques [13,14], probe-based signal enhancement techniques [15,16], temperature-humidity technique [17]

and fluidic control techniques [18]. However, these techniques need either high-cost chemical reagents [13,15], external equipment [17] or complex fabrication with multiple-step operation [18]. In contrast, rapid and simple concentration of fixed sample volume prior to detection, especially for quantitative detection, would be more desirable for sensitivity enhancement, especially for targets with extremely low concentration, such as bacterium [12], viruses [11] and heavy metal ions in contaminated water [3,19] or urine sample [20]. Recently, several studies have reported the integration of various paper-based sample concentration techniques into LFAs [21–23]. For instance, paper-based isotachopheresis (ITP) has been used for simultaneous separation and concentration of goat anti-mouse IgG based on their electrophoretic mobility, which yielded 400-fold signal enhancement in LFAs [21]. However, this technique requires external electrical power, which might not be suitable for use in remote settings. In other studies, aqueous two-phase system (ATPS) has been integrated into LFAs with the use of polyethylene glycol (PEG) for concentration of transferring and Triton X-114 for concentration of *Plasmodium lactate dehydrogenase* for malaria diagnostics [22,23]. However, the former requires extra step of buffer addition [22], while the latter retains the viscous micelle-rich phase near the bottom of the vertically placed strip, which will affect the downstream analysis and thus make the process more

* Corresponding author at: School of Life Sciences, Northwestern Polytechnical University, Xi'an 710072, PR China

** Corresponding author at: The Key Laboratory of Biomedical Information Engineering of Ministry of Education, School of Life Science and Technology, Xi'an Jiaotong University, Xi'an 710049, PR China

E-mail addresses: kittyjh@nwpu.edu.cn (H. Yang), fengxu@mail.xjtu.edu.cn (F. Xu).

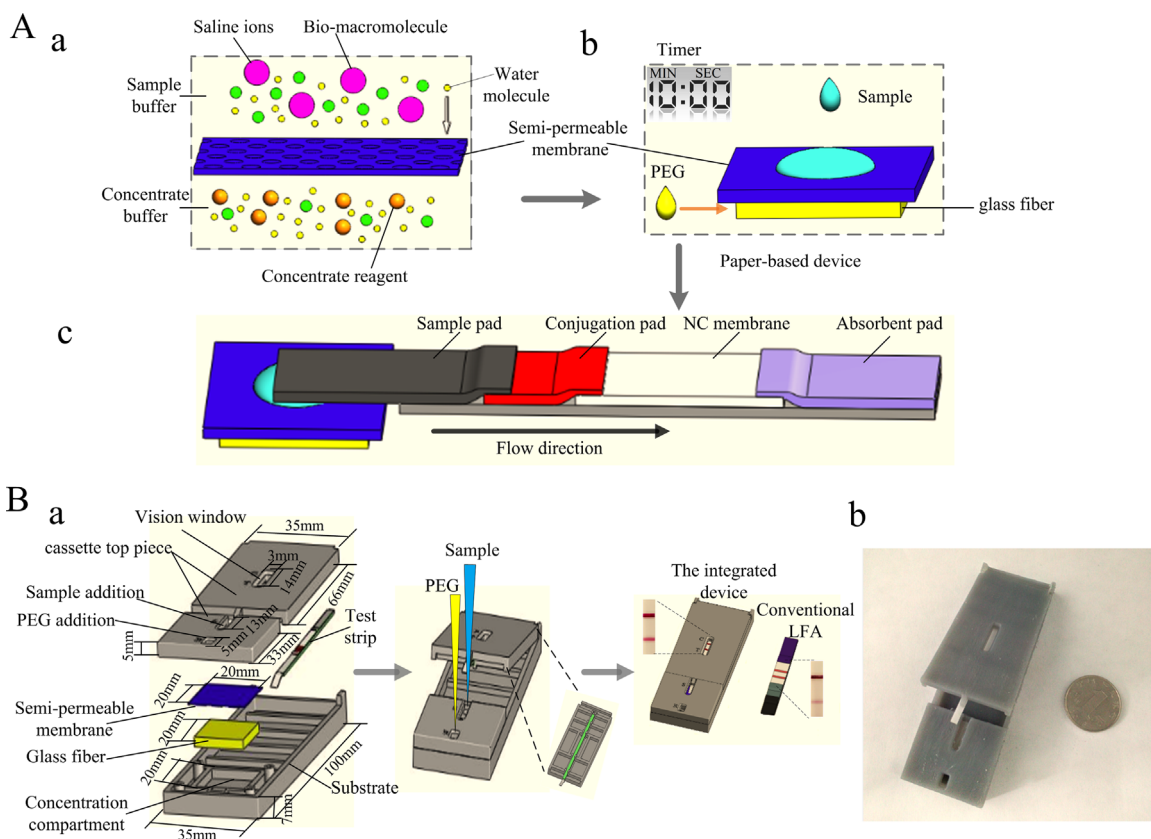


Fig. 1. Schematic of the integrated device. (A) a-the working principle of dialysis concentration; b-paper-based concentration device; c-the integrated device is composed of paper-based concentration device and test strip. (B) a-some details about the prototype device, b-the 3D-printed integrated device of paper-based concentration device and lateral flow strip.

complicated [23]. Therefore, there is still an unmet need for a simpler, lower-cost, and portable concentration method, which can be easily integrated with LFAs.

Dialysis method has been commonly used to remove small molecules from sample solution while keeping large molecules to achieve the concentrated targets for subsequent test [24,25]. Since concentration method based on dialysis is simple, low-cost and portable, it has been integrated into microfluidic chips to concentrate Human Immunodeficiency Virus (HIV) from whole blood, followed by detection with conventional real-time polymerase chain reaction (RT-PCR) [26]. However, integrating dialysis-based concentration method into LFAs for POC applications with enhanced sensitivity has not been explored yet.

To address the poor sensitivity of LFAs with simple, portable and cost-effective method, in this study, we demonstrated for the first time the integration of dialysis method into LFAs for highly sensitive detection of targets. PEG was selected as a dialysate due to its good hygroscopic property [27]. We successfully achieved sample concentration and detection by integrating semi-permeable membrane, glass fiber and PEG buffer into LFAs (Fig. 1A). We further developed a 3D-printed lateral flow device to achieve both target concentration and detection in a single test strip (Fig. 1B). Our device successfully achieved 10-fold signal enhancement in nucleic acid detection (using HIV as a template analyte) and 4-fold antigen detection (using myoglobin (MYO) as a template analyte). Compared to the traditional concentrate methods (e.g., ultrafiltration concentration [28]), our device used paper and semi-permeable membrane to achieve target concentration, which was rapid, simple and equipment-independent. Meanwhile, this integrated device was low-cost, easy-to-use and portable. This technique offers great potential for highly sensitive detection of a broad range of target analyte in POC settings.

2. Experimental

2.1. Chemicals and materials

$\text{HAuCl}_4 \cdot 4\text{H}_2\text{O}$ was supplied by Sinnopharm Chemical Reagent Co., Ltd. (Shanghai, China). PEG8000, semi-permeable membrane (molecular weight cutoff (MWCO): 3.5KD and 8–14KD) and trisodium citrate were supplied by Amersco, LLC (Solon, OH, USA). Sucrose was supplied by ALADDIN Reagent Co., Ltd. (Shanghai, China). Bovine serum albumin (BSA), casein, trehalose, phosphate buffer saline (PBS, pH7.4, 0.01 M) and sodium dodecyl sulfate (SDS) were purchased from MP Biomaterials, LLC (Solon, OH, USA). Polyvinylpyrrolidone (PVP), Tween 20, Triton X-100, Tris (2-carboxyethyl)-phosphine (TCEP) and streptavidin were supplied by Sigma-Aldrich (St. Louis, Mo, USA). Trisodium phosphate, ethylene diamine tetraacetic acid (EDTA), sodium chloride were supplied by Tianli Chemical reagent Co., Ltd. (Tianjin, China). $20 \times \text{SSC}$ buffer was supplied by Ambion Co., Ltd. (USA). Based on the sequences from our early study [15], all the HIV probes were synthesized from Sangon Biotechnology Co., Ltd. (Shanghai, China). Anti-mouse (goat) IgG polyclonal antibody, MYO antibody and antigen were provided by Fapon Biotech Inc. (Shenzhen, China). All the materials for fabricating lateral flow test strip: nitrocellulose membrane (Millipore HFB18002, HFB13502S25, USA), backing pad, absorbent pad, conjugate pad and sample pad, were purchased from Jie ning Biotech Co., Ltd. (Shanghai, China). All chemicals used in this study were analytical reagent grade. All other solutions were prepared with ultrapure water ($> 18 \text{ M}\Omega$) from the Barnstead Nanopure ultrapure water purification system (Thermo Scientific, MA, USA). Amicon ultrafiltration Tube (0.5 mL, 3 K) (Merck Millipore, Germany).

2.2. Preparation of gold nanoparticles (AuNPs), AuNPs modified with HIV detection probe and MYO antibody

AuNPs with average the diameter 13 nm and 30 nm were prepared according to the reported method with slight modifications [29]. Firstly, all glassware and a magnetic stir bar used in this preparation was thoroughly cleaned in the sulfochromic mixture over six hours and then rinsed in distilled water and ultrapure water before using. Then, a 250 mL three-neck round bottom flask was filled with 100 mL of ultrapure water, which connected to a condenser and two stoppers, and placed on a magnetic stirring heater. After boiling, 4.5 mL of 1% trisodium citrate (1 mL needed for 30 nm) was added with vigorously stirring. After 3 min, 1.2 mL of 0.825% chloroauric acid (1.21 mL needed for 30 nm) was added to the solution. The color of the solution immediately changed from pale yellow to blue and then to purple, and finally to red. After 20 min, the heating was turned off and the solution was cooled to room temperature with stirring, and then was stored at 4 °C for further use.

AuNPs (diameter of ~13 nm) modified with HIV detector probe were prepared according to the literature with slight modification [15]. The detail of process was as follows. The detector probe (DP) was thiolated and then activated by adding 20 μ L of 500 mM acetate buffer (pH 4.76), 4 μ L of 10 mM TCEP and 100 μ L of ultrapure water to achieve a final concentration of 100 μ M. After 1 h at room temperature, the 124 μ L of detection probe was added into 20 mL of the AuNPs solution for 16 h at room temperature. Next, 1% SDS was added to obtain the final concentration of 0.01%. After 1 h, the certain volume of 2 M NaCl was added to achieve a final concentration of 160 mM. The solution was then kept at room temperature for 24 h and the supernatant was discarded following the centrifugation at 14000 g for 15 min. The sedimentation was redispersed in elute buffer containing 20 mM Na_3PO_4 , 5% BSA, 0.25% Tween 20, and 10% sucrose, respectively.

AuNPs with diameter of ~30 nm were modified with MYO-antibody as follows: 5 μ L of 0.2 M K_2CO_3 and 12 μ g of antibody were added to 1 mL of the AuNPs solution for incubation 30 min at room temperature. A certain volume of 10% BSA was added to obtain a final concentration of 0.1%. After 10 min, the supernatant solution was removed by centrifugation at 14000 g, 10 min. The sedimentation was redispersed in certain microliter of elute buffer containing 0.85% Tris, 1% BSA, 20% sucrose and 5% trehalose, respectively.

2.3. Fabrication of lateral flow test strips

To immobilize capture and control probes of HIV on NC membrane, these probes were firstly dissolved in streptomycin solution. Similarly, the capture and control antibody of MYO were diluted with coating buffer (2% trehalose in 0.01 M PBS) to 1.5 mg/mL and 1.0 mg/mL, respectively. Then capture and control probes (antibody) were drawn on NC membrane (nucleic acid-HFB18002, protein-HFB13502S25) by XYZ Rapid test dispenser HM3030 (Shanghai kinbio Tech Co., Ltd, China), and kept at 37 °C for 2 h. Next, nitrocellulose (NC) membrane (20 mm \times 2.5 mm), absorbent pad (25 mm \times 2.5 mm), conjugate pad (10 mm \times 2.5 mm) and sample pad (15 mm \times 2.5 mm) were sequentially mounted on a plastic adhesive backing pad with 2 mm overlap between each two adjacent pads. These were termed as "Conventional LFAs". The as-assembled pads were cut into strips with of 2.5 mm by Rapid test cutter ZQ2000 (Shanghai kinbio Tech Co., Ltd, China). As for the conventional LFA assay, different volumes (100 μ L of HIV nucleic acid and 80 μ L of MYO protein) of the sample solution was dispensed onto the sample pad by using a pipette, followed by conventional LFAs detection (**Movie S1 in ESI**). The result of detection can be seen with naked eye within

15 min. For quantitative analysis, the images were captured by mobile phone and the optical density of the test line was analyzed by APP.

Supplementary material related to this article can be found online at <http://dx.doi.org/10.1016/j.talanta.2016.02.017>.

2.4. Fabrication of sample concentration device

The sample concentration device consisted of a glass fiber containing PEG buffer and semi-permeable membrane (**Fig. 1A**). In the device, the MWCO of semi-permeable membrane was 3.5 KD. Both glass fiber and semi-permeable membrane were cut into size of 20 mm \times 20mm, and the PEG buffer was dispensed onto the three layers of glass fiber. The semi-permeable membrane was placed on top of the glass fiber.

2.5. Integration of paper-based sample concentration device into LFAs

The integrated device was designed by Solidworks, which were composed of substrate, fixed cassette top piece, mobile cassette top piece, glass fiber, semi-permeable membrane and test strip (**Fig. 1B(a)**). This integrated device was then printed by a 3D-printer (Formlabs Co., Ltd, USA) using photopolymer resin (Formlabs Co., Ltd, USA) (**Fig. 1B(b)**). The size of the integrated device was 100 mm \times 35 mm \times 12 mm, which was composed of a fixed cassette top piece (33 mm \times 35 mm \times 5 mm) and a mobile cassette top piece (66 mm \times 35 mm \times 5 mm), for target concentration and detection, respectively. The concentration compartment (20 mm \times 20 mm) is consisted of semi-permeable membrane (20 mm \times 20 mm) and glass fiber (20 mm \times 20 mm), with two openings on the cassette, with the sizes of 5 mm \times 3 mm and 13 mm \times 3 mm for adding the PEG buffer and sample, respectively before the assay begins. The detection compartment has a vision window (14 mm \times 3 mm) and the test strip. The test strip was placed at the upper side of the inner detection cassette compartment, supported by the inner supporting frame. According to the specification of the 3-D printer, the accuracy and precision was 0.025 mm. To confirm the accuracy of the fabricated device, we compared the size of each compartment of the printed device with that of the desired size. To confirm the accuracy of the fabricated device, we measured the size of the compartment of three printed devices. The materials of strip, including nitrocellulose (NC) membrane (20 mm \times 2.5 mm), absorbent pad (25 mm \times 2.5 mm), conjugate pad (10 mm \times 2.5 mm) and sample pad (LFAs with the integrated device: 20 mm \times 2.5 mm). As for the integrated device, different volumes (100 μ L of HIV nucleic acid and 80 μ L of MYO protein) of sample solution were vertically added onto the semi-permeable membrane by pipette followed by sample concentration prior to LFAs (**Movie S2 in ESI**). After 10 min sample concentration, the test strip was contacted with the semi-permeable membrane containing sample solution for detection. The result of detection can be seen through vision window within 15 min. For quantitative analysis, the images were captured by mobile phone and the optical density of the test line was analyzed by APP.

Supplementary material related to this article can be found online at <http://dx.doi.org/10.1016/j.talanta.2016.02.017>.

2.6. Optimization assay

We firstly optimized the sample volume of HIV nucleic acid (20 μ L, 30 μ L, 40 μ L, 100 μ L, 110 μ L and 120 μ L) and MYO protein (20 μ L, 30 μ L, 40 μ L, 80 μ L, 90 μ L, 100 μ L and 110 μ L). We then investigated the effect of different sample concentration period (0 min, 3 min, 5 min, 7 min, 10 min, 15 min and 20 min). We also optimized the assay with different volume ratio of sample/PEG for

HIV nucleic acid (1:1, 1:5, 1:7, 1:10 and 1:12) and MYO protein (1:1, 1:5, 1:7 and 1:10).

2.7. Sensitivity assay for nucleic acid and protein detection with the integrated device

To investigate the sensitivity of LFAs with the integrated device, we tested the device with different concentrations of HIV nucleic acid (25 nM, 10 nM, 5 nM, 2.5 nM, 1 nM, 0.5 nM, 0.25 nM, 0.1 nM and 0.05 nM) and MYO protein (100 ng/mL, 50 ng/mL, 25 ng/mL, 12.5 ng/mL, 6.25 ng/mL, 3.12 ng/mL, 1.56 ng/mL, 0.78 ng/mL, 0.39 ng/mL and 0.195 ng/mL).

2.8. The accuracy of the method

To verify the accuracy of the method, we compared the concentration method using our integrated device (paper-based dialysis concentration method) with the conventional ultrafiltration concentration method (Amicon ultrafiltration Tube (0.5 mL, 3 K)). We tested the sensitivity of LFAs with different concentration of HIV nucleic acid (25 nM, 10 nM, 5 nM, 2.5 nM, 1 nM, 0.5 nM, 0.25 nM, 0.1 nM and 0.05 nM) and MYO protein (100 ng/mL, 50 ng/mL, 25 ng/mL, 12.5 ng/mL, 6.25 ng/mL, 3.12 ng/mL, 1.56 ng/mL, 0.78 ng/mL, 0.39 ng/mL and 0.195 ng/mL) according to the reported cross-validation method [30]. Their optical densities were also compared.

3. Results and discussions

In this study, we integrated dialysis method into paper-based device for sample concentration prior to LFAs detection (Fig. 1A). PEG was selected as a dialysate due to its good hygroscopic property for selective absorbing of the small molecules (e.g., water molecule and saline ion) from sample solution by enabling them to diffuse across the selective semi-permeable membranes (Fig. 1A (a)). To use this simple way to achieve dialysis-based concentration on paper, a glass fiber, semi-permeable membrane and PEG solution were used to create a paper-based concentration device for sample concentration (Fig. 1A(b)). Upon 10 min of sample concentration, the test strip was connected to the paper-based concentration device by allowing the sample pad of test strip to be in contact with the semi-permeable membrane containing the sample solution (Fig. 1A(c)). The concentrated sample solution was then bound to the AuNPs-DPs or AuNPs-mcAbs and wicked through the test strip by capillary force, producing colorimetric signal after being captured by the capture probe or antibody on the test strip respectively.

To integrate paper-based concentration device into LFAs, we created an all-in-one paper diagnostic strip that concentrates and detects the target analyte (Fig. 1B). The substrate, semi-permeable membrane, glass fiber and test strip were assembled according to Fig. 1B(a). The cassette was composed of concentration and detection compartments. The concentration compartment consisted of semi-permeable membrane and glass fiber, where glass fiber was filled with saturated PEG buffer solution. The test strip was placed at the upper side of the inner detection cassette compartment (Fig. 1B(a)). The PEG buffer and sample solution were added sequentially through the corresponding inlet holes on the cassette (Fig. 1B(a)). After concentration for 10 min, the test strip was connected to the semi-permeable membrane in the concentration compartment and finally produced a colorimetric signal (Fig. 1B (b)). In the integrated device, the design parameter of integrated device was suitable for the 3D-printer, because the size of device (100 mm × 35 mm × 12 mm) was less than the maximal printed sizes (125 mm × 125 mm × 165 mm), the minimum size of PEG

addition hole of the device (5 mm × 3 mm) was larger than the minimum printed size of the printer (0.3 mm). To confirm the accuracy of the fabricated device, we measured the model size after printing. We found that the size of the printed device was 100.2 mm × 35.3 mm × 12 mm, the concentration compartment was 20.1 mm × 20.1 mm, which was close to the actual size of each compartment. Furthermore, we also found that the small error (0.1–0.3 mm) did not affect the detection sensitivity of integrated device through the experiment result (Data not shown). To confirm the precision of the device, we compared the sizes of three printed devices. We found that their sizes were not significant differences (Data not shown), which were close to each other. The data proved that the printing technique used in device fabrication was accurate and precise.

We also optimized different types of NC membranes suitable for LFAs in terms of the sensitivity of the assay (data not shown), based on which HF180 and HF 135 NC membranes were selected for HIV nucleic acid detection and MYO protein detection, respectively. In conventional LFAs, we found that the ranges of sample volume for proper working were 30–100 μL for HF180 NC membrane (Figure S1A) and 30–80 μL for HF 135 NC membrane (Figure S1B). At low volume of sample (< 30 μL), there was also no signal produced in LFAs due to the inadequate sample to wick through the whole nitrocellulose membrane. At larger volume (> 80–100 μL), there was also absence of signal, mainly because the flow rate of solution was faster than that of nanoparticles, which disallowed AuNPs-DP to completely wick through the nitrocellulose membrane and being captured by the capture probes. Therefore, we chose the optimum 100 μL of HIV nucleic acid and 80 μL of MYO protein for LFAs.

To investigate the effect of integrating semi-permeable membrane into LFAs on the concentration efficiency of target analyte and thus LFAs signal, we performed the assay using 3.5 KD MWCO of semi-permeable membrane without PEG buffer, termed “without PEG”, for HIV nucleic acid (MW of 17.49 KD, 25 nM) and MYO protein (16.7 KD, 25 ng/mL) as model nucleic acid and protein analyte, respectively. We found that LFAs with semi-permeable membrane produced greater signal as compared to conventional LFAs, as indicated by significantly higher fold of optical density, 1.99-fold for HIV and 2.13-fold for MYO detection as compared to conventional LFAs (Fig. 2A). According to Washburn equation [31,32] ($L^2 = \gamma Dt / 4\mu$, L -distance of liquid penetrate, which depended on t), t -time, D -average pore diameter, γ -effective surface tension and μ -viscosity), the flow rate (L/t) of solution was directly proportional to driving force (γ) exerted at the liquid column in the paper strip. In conventional LFAs, the sample solution was continuously added onto the sample pad by pipetting, which induced additional pumping power to drive the liquid flow in the paper strip in addition to the capillary force (Fig. S2A). As for the integrated LFAs, the sample solution was first added into the semi-permeable membrane for 10 min to achieve concentration prior to detection. In this case, the flow of concentrated sample solution was not aided by pipette but only driven by the capillary force (Fig. S2B). Hence, the liquid flow rate in integrated LFAs was slower than the conventional LFAs (Movie S3 in ESI), where slower flow rate has been reported to give better mixing of solution and thus enhanced sensitivity of the assay [18]. Besides, we also found that in LFAs “without PEG”, the concentration period (within 10 min) did not affect the signal of the assay (Fig. 2B), which was straightforward to understand since there was no concentration process. Additionally, it had been reported that the length of paper would also influence the liquid flow rate [33]. As the integrated device consisted of an additional piece of semi-permeable membrane, its entire length (82 mm) was longer than the conventional test strip (60 mm), which allowed longer time for solution mixing and thus improved assay sensitivity.

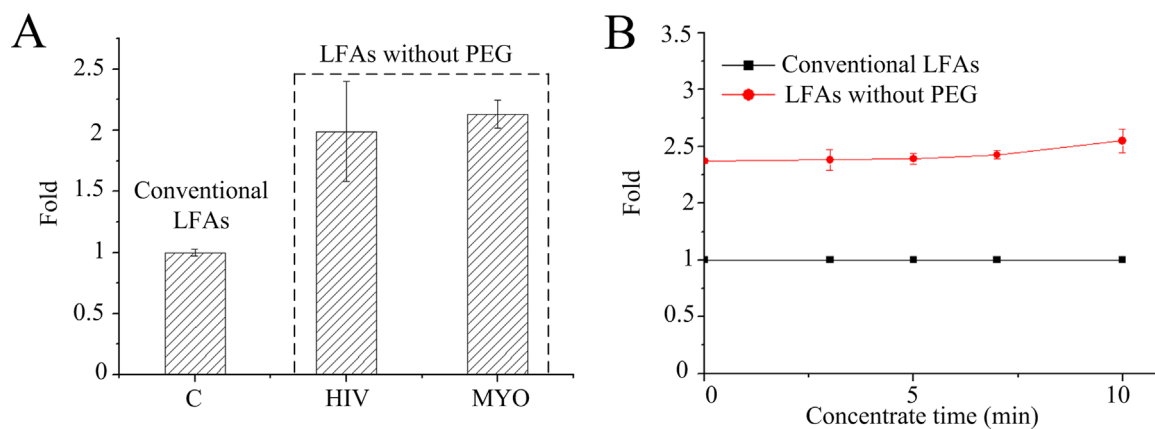


Fig. 2. Comparison between LFAs “without PEG” and conventional LFAs. (A) The signal of LFAs without PEG is higher than conventional LFAs. (C: Conventional LFAs) (B) The no significance effect of the assay signal without PEG after the concentrate period.

Supplementary material related to this article can be found online at <http://dx.doi.org/10.1016/j.talanta.2016.02.017>.

To obtain the highly efficient sample concentration, we optimized the concentration period and the volume ratio of sample/PEG, termed “with PEG”, which were the two main factors affecting the concentration process. We firstly performed concentration for 0 min, 3 min, 5 min, 7 min, 10 min, 15 min and 20 min, respectively. We observed that the signal increased with increasing concentration period and the optimal LFAs signal density was achieved at 10 min, after which there was no significant change (Fig. 3A). To investigate the effect of sample/PEG volume ratio, we performed the assay with a fixed sample volume (100 μ L HIV target) and different volume ratio of sample/PEG 1:1, 1:5, 1:7,

1:10 and 1:12 (Fig. 3B). We observed that the signal of LFAs was gradually enhanced with increasing sample/PEG volume ratio and the optimal signal was achieved at volume ratio of 1:10, as indicated by the significantly higher signal enhancement as compared to the conventional LFAs. Similar results were obtained for detection of MYO, where the optimal sample/PEG volume ratio was 1:7 (Fig. 3C). Further increase in volume ratio of sample/PEG (e.g., 1:12 for HIV, 1:10 for MYO) resulted in a failure of the solution to wick through the test strip. In this case, the sample solution left was less than minimal volume of solution (30 μ L) required to completely wick through the test strip after the concentration process (Fig. S1C). These results showed that with fixed sample volume, the increasing of PEG buffer solution will enhance the

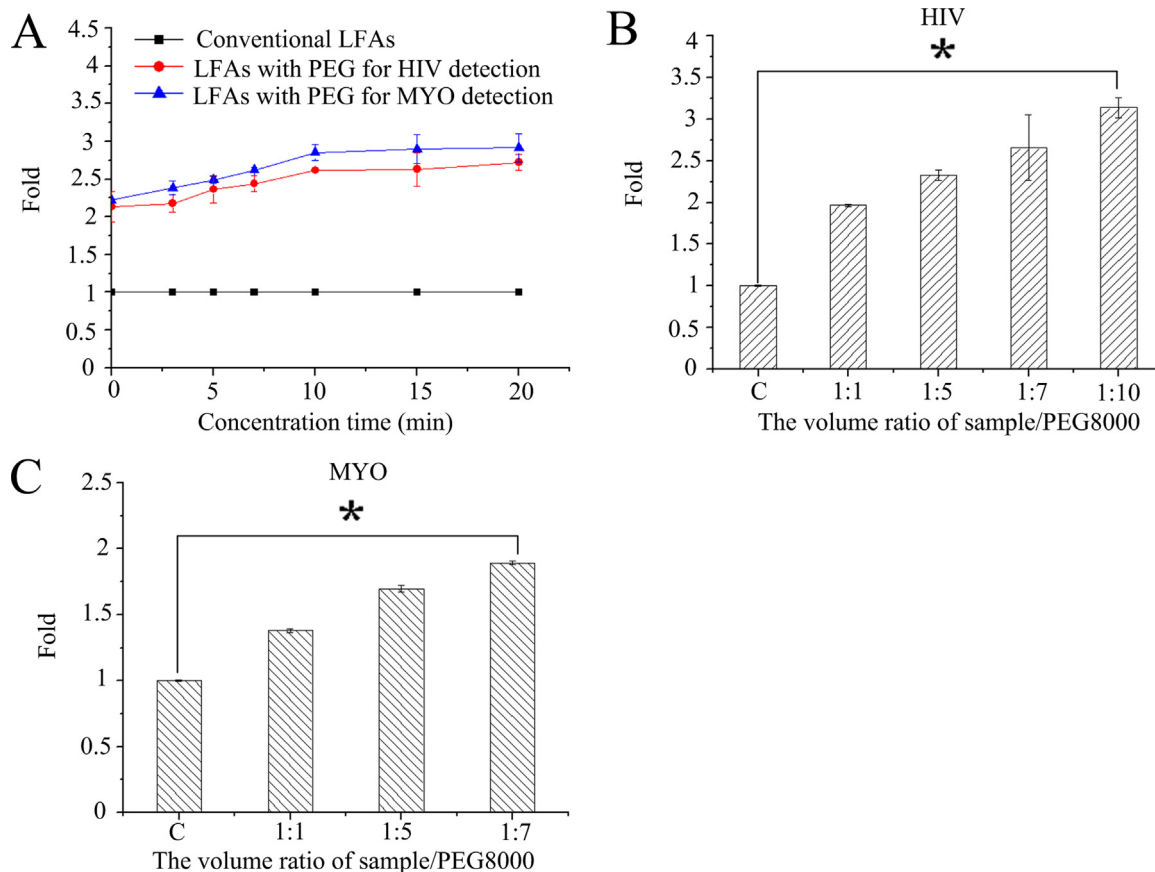


Fig. 3. Optimization of integrated LFAs. Optimization of (A) the concentration time had the effect on LFAs signal. The optimal signal was achieved at volume ratio of sample/PEG 1:10 (B) in nucleic acid (HIV) detection and the volume ratio of 1:7 in (C) antigen (MYO) detection. (C: Conventional LFAs; *: $p < 0.05$).

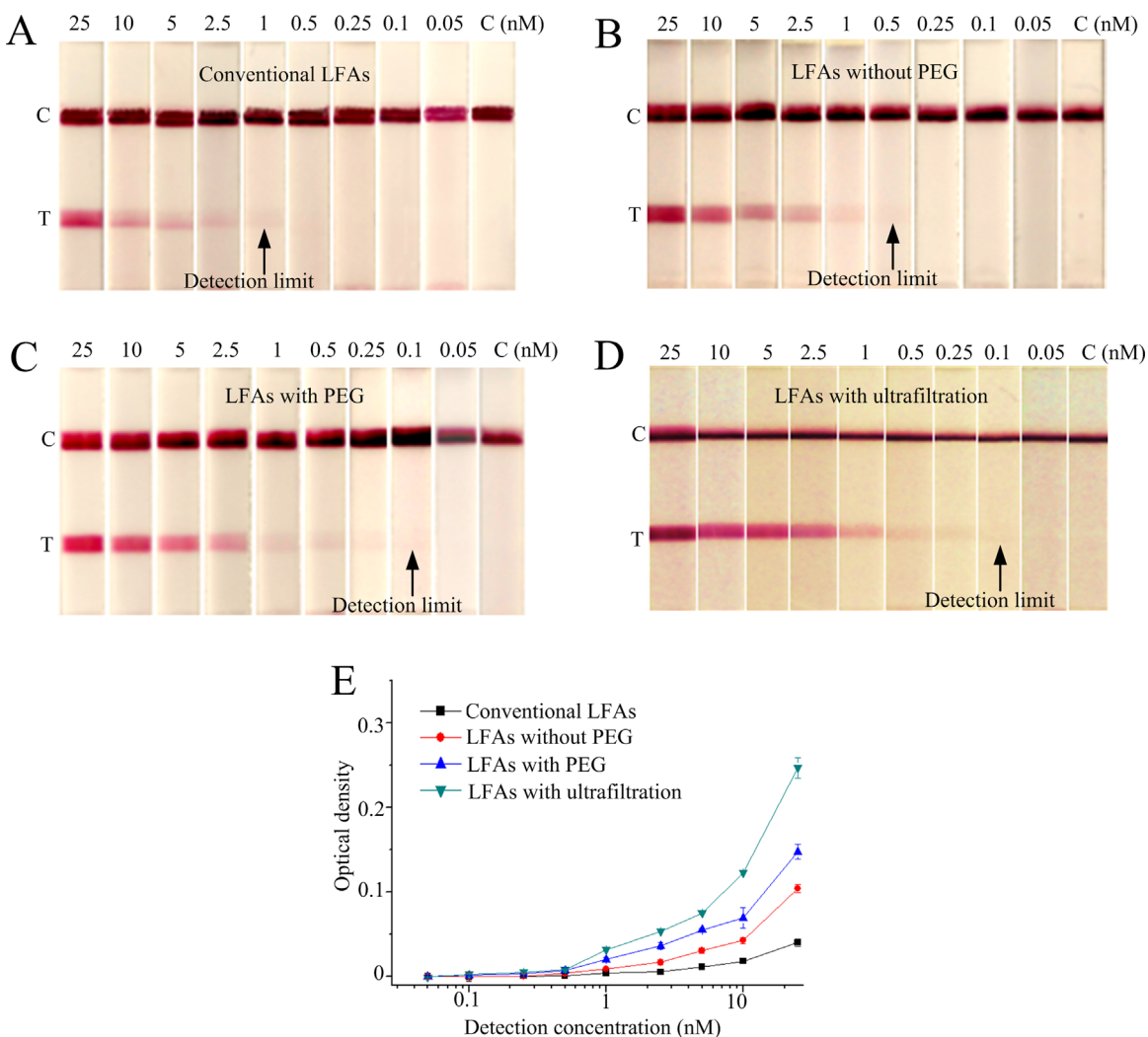


Fig. 4. Detection of HIV with the integrated paper-based device. (A) Conventional LFAs detected HIV at 1 nM. (B) LFAs without PEG detected HIV at 0.5 nM and achieved 2-fold improvement in the detection limit of HIV nucleic acid. (C) LFAs with PEG (Sample/PEG volume ratio of 1:10) successfully detected HIV at 0.1 nM and achieved 10-fold improvement in the detection limit of HIV nucleic acid. (D) LFAs with ultrafiltration detected HIV at 0.1 nM and achieved 10-fold improvement in the detection limit of HIV nucleic acid. (E) The optical density of test line in HIV detection. (C: Control).

concentration effect, and eventually the signal of the assay.

To evaluate the ability of our integrated device to concentrate and detect nucleic acid, we tested the sensitivity of LFAs without PEG and with PEG (Sample/PEG volume ratio of 1:10) using different concentrations of HIV DNA (Fig. 4). We found visually that the color intensity of test line increased with increasing DNA concentration for all three groups of LFAs. The detection limit of conventional LFAs was 1 nM (Fig. 4A), while that of LFAs without PEG was 0.5 nM representing 2-fold sensitivity enhancement. As mentioned, this might be due to the flow delay induced by the presence of semi-permeable membrane which increase the interaction time between the target and AuNPs-DPs, and the binding between AuNPs-DP-target and capture probe, hence enhancing the optical density of the test line (Fig. 4B). As for LFAs with PEG, the detection limit was 0.1 nM, demonstrating 10-fold sensitivity enhancement over the conventional LFAs. This might be due to the flow delay in combination with the concentration effect of PEG, which further enhanced the interaction between the capture probe and AuNPs-DP-target, and thus the optical density of the test line (Fig. 4C). On the other hand, the ultrafiltration concentration method was used to test the sensitivity of LFAs with different concentration of HIV and verify the accuracy of the method. We also found that the sensitivity of LFAs was 0.1 nM

(HIV) (Fig. 4D). We found that the sensitivity of LFAs with the integrated device and the ultrafiltration method were similar based on the intensities of the test line observable by naked eye and the optical densities. Similar to the data of conventional ultrafiltration concentration method, we found that the higher the concentration of the target, the higher the optical densities of the test line, where the optical density was directly proportional to the number of binding between AuNPs-DP-target and capture probe (Table S1 & Fig. 4E).

To check the ability of our integrated device to concentrate and detect protein, we tested the sensitivity of LFAs “without PEG” and LFAs “with PEG” (Sample/PEG volume ratio of 1:7) using different concentrations of MYO protein (Fig. 5). We visualized that the color intensity of test line increase with the increasing protein concentration for all three groups of LFAs. Similar to nucleic acid detection, the detection limit of conventional LFAs was 6.25 ng/mL (Fig. 5A), while that of LFAs without PEG was 3.12 ng/mL (Fig. 5B), representing 2-fold sensitivity enhancement. Using LFAs with PEG, the detection limit was 1.56 ng/mL, and demonstrating 4-fold sensitivity enhancement over the conventional LFAs (Fig. 5C). We also compared the sensitivity of LFAs with the ultrafiltration concentration method and our integrated LFA. We found that the sensitivity of LFAs was 1.56 ng/mL using both methods (Fig. 5D).

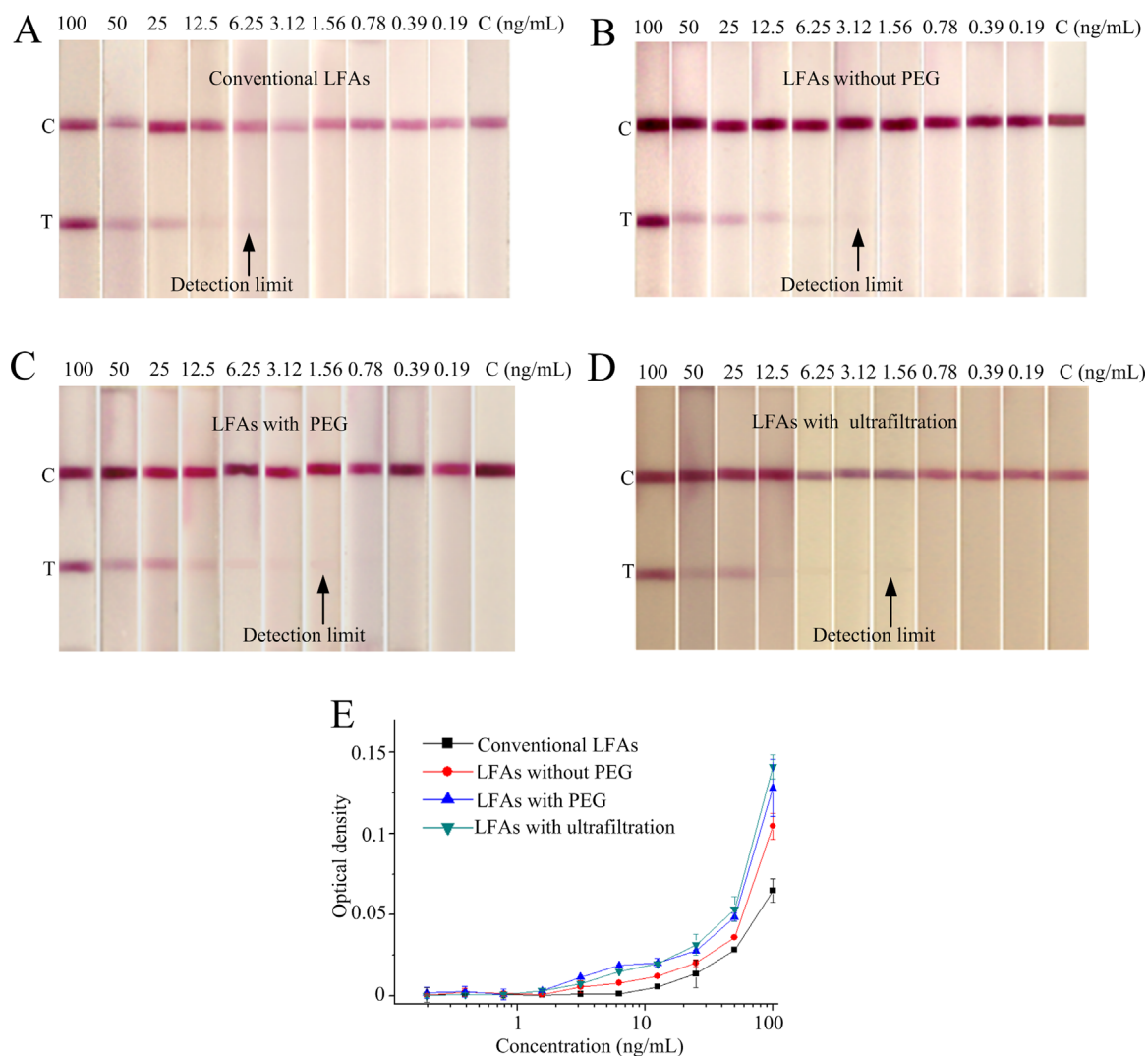


Fig. 5. Detection of MYO with the integrated paper-based device. (A) Conventional LFAs detected MYO at 6.25ng/mL. (B) LFAs without PEG detected MYO at 3.125ng/mL and achieved 2-fold improvement in the detection limit of MYO protein. (C) LFAs with PEG (Sample/PEG volume ratio of 1:7) successfully detected MYO at 1.56;ng/mL and achieved 4-fold improvement in the detection limit of MYO protein. (D) LFAs with ultrafiltration detected MYO at 1.56 ng/mL and achieved 4-fold improvement in the detection limit of HIV nucleic acid. (E) The optical density of test line in MYO detection. (C: Control).

Additionally, we also found that their detection limits was similar based on the optical densities of the test zone (Table S2 & Fig. 5E).

We successfully demonstrated that our integrated device could detect lower concentration sample and improve the sensitivity of LFAs. Comparison of the proposed concentration and detection method using the integrated device with the existing methods were summarized in Table 1. As compared to ITP-based LFAs [21], our method does not require external power, which is applicable in resource-limited settings. Furthermore, as compared to enzyme-based signal enhancement techniques [13] and probe-based signal enhancement techniques [15], our device offers low cost and simple operation. Thus, we envision that in the future the integration of sample preparation into this platform offers great potential for sensitive detection of various targets in POC settings.

4. Conclusion

In the present study, we successfully developed a new LFAs device by integrating dialysis method into LFAs to concentrate sample for improving the sensitivity of LFAs. The integrated device was able to concentrate and detect target analyte, resulting in 10-fold and 4-fold

sensitivity enhancement in nucleic acid and protein detection, respectively. Unlike traditional methods, our device was performed on paper-based substrate and reduced some complex processes, which was simple, low-cost and portable. This integrated device holds great potential for highly sensitive detection of a broad range of target analyte for medical diagnostics, food safety and environmental monitoring.

Acknowledgments

This work was supported by grants from the Natural Science Foundation of Shaanxi Province (2014JM1002) and the National Natural Science Foundation of China (11472224), and the International Science & Technology Cooperation Program of China (2013DFG02930), National Instrumentation Program of China (2013YQ190467) BP-M and JRC received funding from the Ministry of Higher Education (MOHE), Government of Malaysia under the high impact research (UM.C/HIR/MOHE/ENG/44).

Appendix A. Supplementary material

Supplementary data associated with this article can be found in the online version at <http://dx.doi.org/10.1016/j.talanta.2016.02.017>.

Table 1
The advantages and disadvantages of the integrated device as compared to other methods.

Methods	Advantages	Disadvantages	Reference
The integrated device (Paper-based dialysis concentration of LFAs)	<ul style="list-style-type: none"> · Integrated · No need external power · Portable · 10-fold 	<ul style="list-style-type: none"> · Need PEG buffer · Low cost 	In this study
ITP-based LFAs	<ul style="list-style-type: none"> · 1000-fold 	<ul style="list-style-type: none"> · Need external power · Not integrated · Not portable 	[21]
Enzyme-based signal enhancement techniques of LFAs	<ul style="list-style-type: none"> · Integrated · No need instrumentation · Portable · 0.01 pM target DNA 	<ul style="list-style-type: none"> · Complex preparation · Instability (Need enzyme) · High cost 	[13]
Probe-based signal enhancement techniques of LFAs	<ul style="list-style-type: none"> · Integrated · Portable · 2.5-fold 	<ul style="list-style-type: none"> · Need probe · Complex fabrication · High cost 	[15]

References

- [1] J.H. Lee, H.S. Seo, J.H. Kwon, H.T. Kim, K.C. Kwon, S.J. Sim, Y.J. Cha, J. Lee, Multiplex diagnosis of viral infectious diseases (AIDS, hepatitis C, and hepatitis A) based on point of care lateral flow assay using engineered proteinticles, *Biosens. Bioelectron.* 69 (2015) 213–225.
- [2] L. Anfossi, C. Baggiani, C. Giovannoli, G. D'Arco, G. Giraudi, Lateral-flow immunoassays for mycotoxins and phycotoxins: a review, *Anal. Bioanal. Chem.* 405 (2013) 467–480.
- [3] Y. Liu, A. Wu, J. Hu, M. Lin, M. Wen, X. Zhang, C. Xu, X. Hu, J. Zhong, L. Jiao, Y. Xie, C. Zhang, X. Yu, Y. Liang, X. Liu, Detection of 3-phenoxybenzoic acid in river water with a colloidal gold-based lateral flow immunoassay, *Anal. Biochem.* 483 (2015) 7–11.
- [4] R. de la Rica, M.M. Stevens, Plasmonic ELISA for the ultrasensitive detection of disease biomarkers with the naked eye, *Nat. Nanotechnol.* 7 (2012) 821–824.
- [5] P.D. Khot, D.N. Fredricks, PCR-based diagnosis of human fungal infections, *Expert Rev. Anti-infect. Ther.* 7 (2009) 1201–1221.
- [6] G.A. Posthuma-Trumpie, J. Korf, Av Amerongen, Lateral flow (immuno)assays: its strengths, weaknesses, opportunities and threats. A literature survey.pdf >, *Anal. Bioanal. Chem.* 393 (2009) 569–582.
- [7] J.R. Choi, R. Tang, S. Wang, W.A.B.W. Abas, B. Pingguan-Murphy, F. Xu, Paper-based sample-to-answer molecular diagnostic platform for point-of-care diagnostics, *Biosens. Bioelectron.* 74 (2015) 427–439.
- [8] S. Feng, J.R. Choi, T.J. Lu, F. Xu, State-of-Art Advances in Liquid Penetration Theory and Flow Control in Paper for Paper-Based Diagnosis, DOI (2015).
- [9] S. Wang, F. Xu, U. Demirci, Advances in developing HIV – 1 viral load assays for resource-limited settings, *Biotechnol. Adv.* 28 (2010) 770–781.
- [10] F. Mashayekhi, A.M. Le, P.M. Nafisi, B.M. Wu, D.T. Kamei, Enhancing the lateral-flow immunoassay for detection of proteins using an aqueous two-phase micellar system, *Anal. Bioanal. Chem.* 404 (2012) 2057–2066.
- [11] F. Mashayekhi, R.Y. Chiu, A.M. Le, F.C. Chao, B.M. Wu, D.T. Kamei, Enhancing the lateral-flow immunoassay for viral detection using an aqueous two-phase micellar system, *Anal. Bioanal. Chem.* 398 (2010) 2955–2961.
- [12] Y. Terao, T. Yonekita, N. Morishita, T. Fujimura, T. Matsumoto, F. Morimatsu, Potential rapid and simple lateral flow assay for *Escherichia coli* O111, *J. Food Prot.* 76 (2013) 755–761.
- [13] Yuqing He, Sanquan Zhang, Xibao Zhang, Meenu Balod, Anant S. Gurung, Hui Xu, Xueji Zhang, G. Liu, Ultrasensitive nucleic acid biosensor based on enzyme-gold nanoparticle dual label and lateral flow strip biosensor, *Biosens. Bioelectron.* 26 (2011) 2018–2024.
- [14] J. Hu, S. Wang, L. Wang, F. Li, B. Pingguan-Murphy, T.J. Lu, F. Xu, Advances in paper-based point-of-care diagnostics, *Biosens. Bioelectron.* 54 (2014) 585–597.
- [15] J. Hu, L. Wang, F. Li, Y.L. Han, M. Lin, T.J. Lu, F. Xu, Oligonucleotide-linked gold nanoparticle aggregates for enhanced sensitivity in lateral flow assays, *Lab on a Chip* 13 (2013) 4352–4357.
- [16] D.H. Choi, S.K. Lee, Y.K. Oh, B.W. Bae, S.D. Lee, S. Kim, Y.B. Shin, M.G. Kim, A dual gold nanoparticle conjugate-based lateral flow assay (LFA) method for the analysis of troponin I, *Biosens. Bioelectron.* 25 (2010) 1999–2002.
- [17] J.R. Choi, J. Hu, S. Feng, W.A. Wan Abas, B. Pingguan-Murphy, F. Xu, Sensitive biomolecule detection in lateral flow assay with a portable temperature-humidity control device, *Biosens. Bioelectron.* 79 (2015) 98–107.
- [18] L. Rivas, M. Medina-Sanchez, A. de la Escosura-Muniz, A. Merkoci, Improving sensitivity of gold nanoparticle-based lateral flow assays by using wax-printed pillars as delay barriers of microfluidics, *Lab on a chip* 14 (2014) 4406–4414.
- [19] V.N. Bulut, D. Arslan, D. Ozdes, M. Soylyk, M. Tufekci, Preconcentration, separation and spectrophotometric determination of aluminium(III) in water samples and dialysis concentrates at trace levels with 8-hydroxyquinoline-cobalt(II) coprecipitation system, *J. Hazard. Mater.* 182 (2010) 331–336.
- [20] M.P. Robert, S. Wallis, Dick Menzies, T. Mark Doherty, Gerhard Walzl, Mark D. Perkins, Alimuddin Zumla, Biomarkers and diagnostics for tuberculosis: progress, needs, and translation into practice, *Lancet* 375 (2010).
- [21] B.Y. Moghadam, K.T. Connelly, J.D. Posner, Two orders of magnitude improvement in detection limit of lateral flow assays using isotachopheresis, *Anal. Chem.* 87 (2015) 1009–1017.
- [22] R.Y. Chiu, E. Jue, A.T. Yip, A.R. Berg, S.J. Wang, A.R. Kivnick, P.T. Nguyen, D. T. Kamei, Simultaneous concentration and detection of biomarkers on paper, *Lab on a Chip* 14 (2014) 3021–3028.
- [23] D.Y. Pereira, R.Y. Chiu, S.C. Zhang, B.M. Wu, D.T. Kamei, Single-step, paper-based concentration and detection of a malaria biomarker, *Anal. Chim. Acta* 882 (2015) 83–89.
- [24] S.M. Andrew, J.A., Z.L. Titus, Dialysis and concentration of protein solutions Appendix 3:A.3H, *Curr. Protoc. Toxicol.* (2002) 1–5.
- [25] L.C. CRAIG, Techniques for the study of peptides and proteins by dialysis and diffusion, *Methods Enzymol.* 11 (1967) 870–905.
- [26] Nga T. Ho, Andy Fan, Catherine M. Klapperich, M. Cabodi, Sample concentration and purification for point-of-care diagnostics, *Ann. Int. Conf. IEEE EMBS* (2012) 2396–2399.
- [27] E. Jameson, N.H. Mann, I. Joint, C. Sambles, M. Muhling, The diversity of cyanomyovirus populations along a North-South Atlantic Ocean transect, *ISME J.* 5 (2011) 1713–1721.
- [28] Y.J. Li, M.J. Ma, J.J. Zhu, Dual-signal amplification strategy for ultrasensitive photoelectrochemical immunosensing of alpha-fetoprotein, *Anal. Chem.* 84 (2012) 10492–10499.
- [29] Y.M. Xun Mao, Aiguo Zhang, Lurong Zhang, Lingwen Zeng, Guodong Liu, Disposable nucleic acid biosensors based on gold nanoparticle probes and lateral flow strip, *Anal. Chem.* 81 (2009) 1660–1668.
- [30] B.M.K. Jamie, R. Wood, Craig Kollman, Roy W. Beck, D. Ph.D., J.P.Y., Callyn A. Hall, Eda Cengiz, Michael J. Haller, G.J.K. Krishna Hassan, William V. Tamborlane, Accuracy and precision of the axis-shield afnion hemoglobin A1c measurement device, *J. Diabetes Sci. Technol.* 6 (2012) 380–386.
- [31] E.W.N. Murilo Santhiago, Glauco P. Santos, Lauro TKubota* Microfluidic paper-based devices for bioanalytical applications, *Bioanalysis* 6 (2014) 89–106.
- [32] Emanuel Elizalde, R. Urteagaa, C.L.A. Berlib, Rational design of capillary-driven flows for paperbased microfluidics Lab on a chip, DOI 10.1039/x0xx00000x 10.1039/b000000x/ 10.1039/C4LC01487A(2015).
- [33] B.J. Toley, B. McKenzie, T. Liang, J.R. Buser, P. Yager, E. Fu, Tunable-delay shunts for paper microfluidic devices, *Anal. Chem.* 85 (2013) 11545–11552.